

Cesiumauride Ammonia (1/1), $\text{CsAu} \cdot \text{NH}_3$: A Crystalline Analogue to Alkali Metals Dissolved in Ammonia?*

Anja-Verena Mudring, Martin Jansen,* Jörg Daniels,
Steffen Krämer, Michael Mehning,
Joao Paulo Prates Ramalho, Aldo Humberto Romero,
and Michele Parrinello

Relativistic contributions to the energy of the electronic states in atoms grow with increasing atomic number, and become comparable to the usual shell structure effects beyond the fifth period. One of the consequences for the electronic structures is the relativistic radial contraction and energetic stabilization of the s shells which has been found to be most pronounced for gold.^[1] Many of the peculiarities in the chemical and physical properties of gold can be traced back directly to this fact. Among others, this holds true for the high electron affinity (the highest of any metal) which explains the propensity of gold to adopt the negative oxidation state -1 . By spectroscopic and, even more convincingly, chemical means it has been shown that this is not a barely formal valence state, but instead true ionic Au^- entities are present, when an appropriate environment is provided. In particular, the formation of the ternary phase Cs_3AuO from CsAu and Cs_2O by interdiffusion in the solid state has given conclusive support to this view.^[2] To provide further evidence for Au^- ions being a stable species we have subject CsAu to an electrolytic dissociation by dissolving it in a polar solvent. Indeed, CsAu dissolves readily in liquid ammonia forming a yellow solution. Surprisingly, on slowly removing ammonia, CsAu was not recovered directly, instead a new, intense blue solid crystallized; with X-ray single-crystal data the structure

was solved and refined, and gave the composition $\text{CsAu} \cdot \text{NH}_3$. As the color is reminiscent of the blue solutions of alkali metals in ammonia,^[3] and as gold(-1) can transfer electron density towards a suitable acceptor,^[4] one could suspect this ammoniate to represent a crystalline analogue to the former electrode solutions.

The properties of cesiumauride ammonia (1/1), $\text{CsAu} \cdot \text{NH}_3$, are governed both by its highly reductive power and its thermal lability. In consequence, the compound is extremely sensitive towards even traces of water or oxidizing agents, for example, atmospheric oxygen. According to thermal analyses (simultaneous differential thermal analysis (DTA) and thermogravimetry (TG)), $\text{CsAu} \cdot \text{NH}_3$ releases ammonia when heated above 225 ± 5 K. Thus, the temperature of decomposition is well below the boiling point of ammonia (239 K) which indicates a moderate interaction of ammonia in the solid. An observed weight loss of 5 % agrees well with the assumed evolution of one mole of NH_3 per mole $\text{CsAu} \cdot \text{NH}_3$.

The crystal structure of $\text{CsAu} \cdot \text{NH}_3$ ^[5] exhibits features characteristic for low-dimensional systems. Slabs of overall composition CsAu are separated by single NH_3 layers. The heavy-atom substructure can be derived from the structure of solvent-free CsAu by cutting out slabs oriented parallel to the crystallographic (110) direction, (Figure 1, left). These two-dimensional units have a thickness of half the unit-cell face diagonal and are separated by NH_3 units. A similar structural motif is found in auride aurates, such as $\text{Cs}_7\text{Au}_5\text{O}_2$, where the same types of slabs are intercalated by AuO_2^{3-} entities.^[6] In $\text{CsAu} \cdot \text{NH}_3$ the gold atoms are shifted towards each other forming zigzag chains with comparatively short Au–Au separations ($d(\text{Au}–\text{Au}) = 302$ pm, c.f. CsAu : $d(\text{Au}–\text{Au}) = 426$ pm,^[7, 8] Table 1), which indicates some bonding interac-

- [*] Prof. Dr. M. Jansen, Dr. A.-V. Mudring
Max-Planck-Institut für Festkörperforschung
Heisenbergstrasse 1
70569 Stuttgart (Germany)
Fax: (+49) 711-689-1502
E-mail: martin@jansen.mpi-stuttgart.mpg.de
- Dr. J. Daniels
Anorganisch-Chemisches Institut
Friedrich-Wilhelms-Universität Bonn, 53121 Bonn (Germany)
- Dr. S. Krämer, Prof. Dr. M. Mehning
2. Physikalisches Institut
Universität Stuttgart, 70550 Stuttgart (Germany)
- Prof. Dr. J. P. Prates Ramalho
Departamento de Química
Universidade de Evora, 7001 Evora codex (Portugal)
- Prof. Dr. A. H. Romero
Facultad de Física
Pontificia Universidad Católica de Chile
Casilla 306, Santiago 22 (Chile)
- Prof. Dr. M. Parrinello^[+]
Max-Planck-Institut für Festkörperforschung
Heisenbergstrasse 1, 70569 Stuttgart (Germany)

[+] new address:
ETH Zurich, Centro Svizzero di Calcolo Scientifico (CSCS)
Via Cantonale, Galleria 2, 6928 Manno (Switzerland)

[**] We gratefully acknowledge financial support by the Fonds der Chemischen Industrie. We thank Dr. O. Oeckler for the single-crystal data collection, E. Brücher and N. Wagner for magnetic measurements.

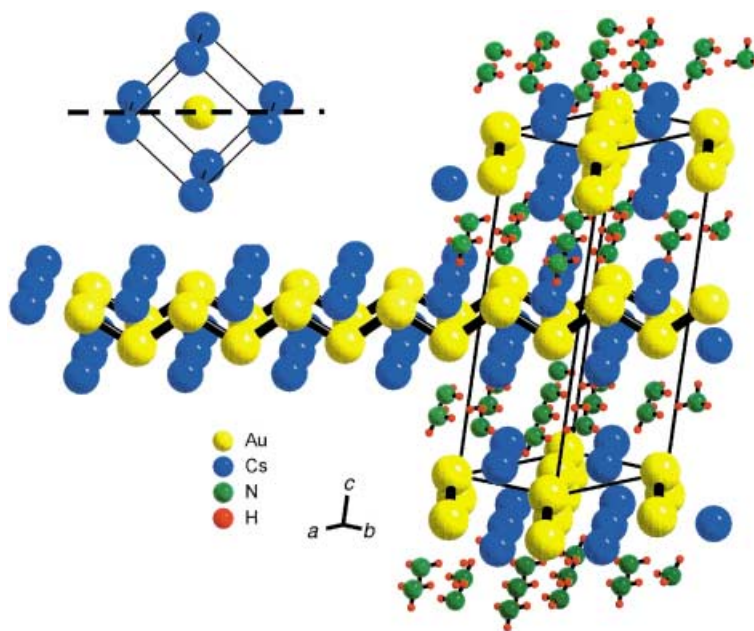


Figure 1. Structure of $\text{CsAu} \cdot \text{NH}_3$. Right: Unit cell. Left: Derivation of the CsAu substructure in $\text{CsAu} \cdot \text{NH}_3$ from CsAu . CsAu , elemental cube (top). $\text{CsAu} \cdot \text{NH}_3$ heavy atom substructure (middle).

Table 1. Interatomic distances in CsAu · NH₃.

	d [pm]		d [pm]
Au–Au	301.5(8)	Cs–N	323(1)
	302(1)		323(2)
Au–Cs	359(2)	Cs–Au	359(2)
	359.7(9)		359.7(9)
	363.2(1)		363.2(1)
	363.3(1)		363.3(1)
	371.7(9)		371.7(9)
	371.7(8)		371.7(8)

tion. The chains are well separated ($d(\text{Au–Au, interchain}) = 504$ pm). The interatomic Cs–Cs distances are elongated ($d(\text{Cs–Cs}) = 479$ pm, c.f. CsAu: $d(\text{Cs–Cs}) = 426$ pm^[7, 8]), while the mean Cs–Au separation ($d(\text{Cs–Au}) = 365$ pm) is just slightly below the value found in CsAu ($d(\text{Cs–Au}) = 369$ pm), Table 1.

Ammonia completes the coordination spheres of the heavy atoms in a way that for both Cs and Au the coordination number (C.N.) of 8 is restored (Figure 2a, b). Each NH₃ bridges two cesium atoms, forming an angle (Cs–NH₃–Cs) of

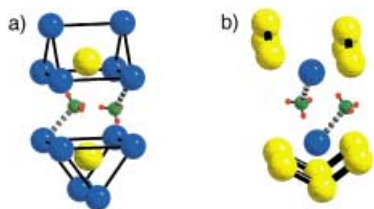


Figure 2. Au (a) and Cs (b) environments in CsAu · NH₃. For color code see Figure 1.

94.73°. The NH₃ lone pair is directed to one of the Cs atoms and, in consequence, it is no longer available for hydrogen bonding. The Cs–N separation of 323 pm is comparable to those found for cesium ammoniates, for example, the polyphosphides.^[9]

The title compound, which can be regarded as an ammoniate of an alloy, is without precedence from a chemical as well as a structural point of view. Thus, no reference systems are available which could serve as a basis for an attempt to understand and classify the properties and their relations to chemical bonding, and further experimental and theoretical work appeared to be necessary to gain insight into the electronic structure of this solid.

A particularly strong tool for probing the 6s electron concentration and distribution, which are assumed to play a key role, is ¹⁹⁷Au Mössbauer spectroscopy. The results give unambiguous evidence for a significant reduction of the electron density at the gold nucleus, as compared to the parent CsAu (Table 2). Taking into account the chemical shift only, the values for CsAu · NH₃ lie between those of RbAu and KAu₂. The modest quadrupole splitting is attributed to the reduced symmetry at the gold site.^[10]

Complementary information regarding the electronic structure of CsAu · NH₃, as obtained by ¹H and ¹³³Cs NMR spectroscopic measurements. NMR spectroscopic data is available on the parent compounds, namely NH₃^[11] and

Table 2. Mössbauer parameters of aurides.

	Chemical shift δ [mm s ⁻¹]	Quadrupole split Δ [mm s ⁻¹]	FWHM [mm s ⁻¹] ^[a]
CsAu · NH ₃	5.96(1)	1.75(2)	1.08(2)
Au (reference)	–1.23	0	0.95
KAu ₂	3.16(3)	4.23(4)	0.73(7)
RbAu	6.70(2)	0	1.31(5)
CsAu	7.00(2)	0	0.96(6)

[a] FWHM = full width at half maximum.

CsAu,^[12–14] on various solutions of alkali metals in ammonia,^[15, 16] and other materials with localized charge inhomogeneities.^[17]

Here we report ¹H (100 MHz, TMS) and ¹³³Cs (50 MHz, CsNO₃) NMR spectroscopy performed on CsAu · NH₃ powder samples as well as ¹H NMR spectroscopy on pure ammonia and ¹³³Cs NMR spectroscopy on CsAu. We have used a home-built pulsed NMR spectrometer and measured spectral lineshapes as well as spin-lattice relaxation rates for temperatures below 200 K down to 5 K.

The ¹H line position, linewidth, and spin-lattice relaxation suggest that the properties of solid ammonia are essentially preserved in CsAu · NH₃. The dynamics of the ammonia molecules can be described in a way similar to those of pure solid NH₃.^[11] The molecules undergo a hindered rotation around their symmetry axis with an activation energy of about 100 meV (4800 kJ mol⁻¹) and a correlation time τ_c^0 of 3.7×10^{-13} s. Above 180 K a sizable narrowing of the ¹H resonance line occurs within a small temperature range of about 5 K. Since this temperature is very close to the melting temperature of pure ammonia we attribute the observed line narrowing to a melting transition in the NH₃ layers.

The ¹³³Cs spectra (Figure 3) for 86 K display a strongly broadened and asymmetrical lineshape with a high-frequency tail which is not observed in pure CsAu. The latter shows a

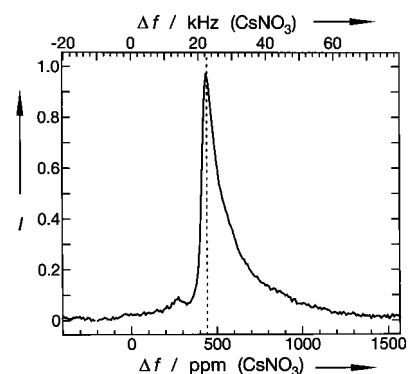


Figure 3. ¹³³Cs NMR spectrum of CsAu · NH₃ at 86 K. The dashed line marks the line position of pure CsAu which exhibits a chemical shift of ca. 420 ppm. The reference is an aqueous 1M CsNO₃ solution.

much narrower, symmetric resonance signal with only a weak temperature dependence between 80 K and 350 K. The frequency of the maximum spectral intensity in CsAu · NH₃ coincides with the spectral line position of CsAu for temperatures between 80 K and 200 K (dashed line in Figure 3). The line broadening clearly is inhomogeneous in character since

the spin-lattice relaxation rates vary over the signal, being sizably enhanced for Cs nuclei showing a large frequency shift. The behavior of both, lineshape and relaxation, can be explained by assuming dilute localized inhomogeneities in electron density on the CsAu chains which induce an additional site-dependent frequency shift and an enhanced fluctuation strength. We note here that the line is not “Knight-shifted” since there is no paramagnetism observed neither in magnetic susceptibility nor in ESR measurements. The observed shift is a result of the chemical shift, which in the case of ^{133}Cs is on the order of 15000 ppm.^[12, 13, 18] The origin of the observed localized inhomogeneities can be attributed to a reduction of the charge density in the Au partial structure by a charge transfer towards the cesium/ammonia regions. Assuming a bipolaron state of spin-paired electrons (charge $2e^-$, spin $S=0$) would explain both the observed NMR spectroscopic behavior of the Cs centers and the diamagnetism of the bulk samples as determined by superconducting quantum interference device (SQUID) measurements. The electron is distributed over several NH_3 molecules. The charge transfer refers to only a few percent of an electron per Au center. The corresponding bipolarons are either randomly distributed or somewhat ordered. This cannot be distinguished at the moment. In any case it leads to a distribution of the chemical shifts of the ^{133}Cs signal as will be elaborated in a separate publication. We note that the effect of a localized charge on NMR spectrum parameters is substantially enhanced for ^{133}Cs nuclei in comparison with ^1H nuclei since the former exhibits large chemical-shift changes induced by the electronic environment a result of an easily polarizable electron shell.^[18]

This way of explaining the experimental results is backed in part by an electronic-structure calculation of $\text{CsAu} \cdot \text{NH}_3$, and, for comparison, of the related compound CsAu . We use the density functional theory (DFT) in the local density approximation (LDA).^[19] For both compounds the internal atomic coordinates were fixed from the experiments and the volume was allowed to vary. The electronic gap between empty and occupied states is a similar value in both compounds, a trend that is likely to be true in spite of the LDA errors. The character of the states at the top of the valence band (HOMO) and at the bottom of the conduction band (LUMO) is shown in Figure 4. In both CsAu (Figure 4a) and $\text{CsAu} \cdot \text{NH}_3$ (Figure 4b) the top of the valence band is a state which is mostly localized on the Au atoms. In contrast the bottom conduction state is located in the interstitial region in CsAu and on the N atom in $\text{CsAu} \cdot \text{NH}_3$.

Further insight into the bonding properties of these compounds can be extracted from the maximally localized Wannier functions.^[20] The spread of the resulting Wannier functions and their Kohn and Sham Hamiltonian expectation value ($\langle w_i | H | w_i \rangle$) are shown in Table 3. For CsAu it turns out that the valence electrons are localized on the gold atom, totally in line with the accepted picture of CsAu as an almost ionic compound, where, because of the difference in electronegativity the Cs electron is transferred to the gold atom. The doubly occupied valence states can be partitioned into two groups; two representative Wannier functions are shown in Figure 5 and exhibit a clear s+d character.

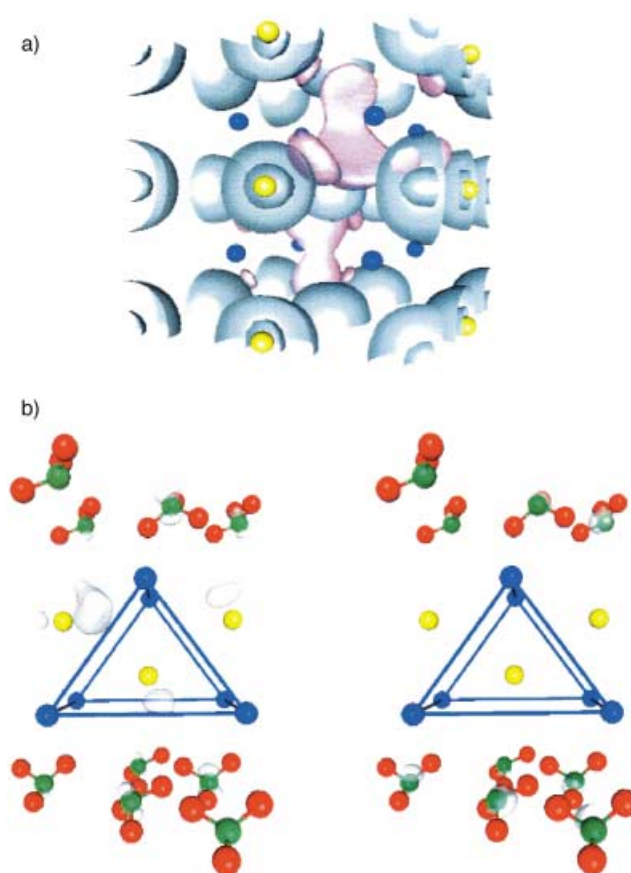


Figure 4. a) HOMO (blue) and LUMO (rose) states of CsAu . b) HOMO (left) and LUMO (right) states of $\text{CsAu} \cdot \text{NH}_3$. For color code see Figure 1.

Table 3. Spread in real space and average energy of the Wannier functions located over a gold atom in $\text{CsAu} \cdot \text{NH}_3$ and CsAu .

State	$\text{CsAu} \cdot \text{NH}_3$		CsAu	
	$S [\text{\AA}]^{\text{[a]}}$	$\langle E \rangle [\text{eV}]^{\text{[b]}}$	$S [\text{\AA}]^{\text{[a]}}$	$\langle E \rangle [\text{eV}]^{\text{[b]}}$
a	0.704	− 5.996	0.705	− 7.943
b	0.712	− 5.965	0.705	− 7.943
c	0.719	− 5.831	0.705	− 7.943
d	0.720	− 5.825	0.770	− 7.775
e	0.726	− 5.734	0.770	− 7.775
f	0.965	− 5.578	0.770	− 7.775

[a] $S = \sum_i (\langle w_i | r^2 | w_i \rangle - \langle w_i | r | w_i \rangle^2)$. [b] $\langle E \rangle = \langle w_i | H | w_i \rangle$.

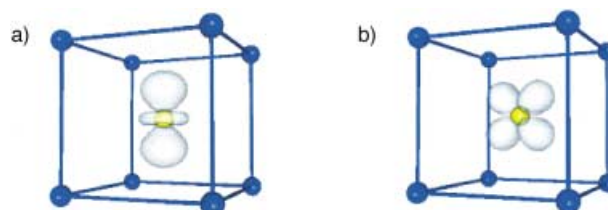


Figure 5. Wannier densities of CsAu . a) Lower energy set of degenerate Wannier states. b) Higher energy set. For color code see Figure 1.

$\text{CsAu} \cdot \text{NH}_3$, in contrast, no longer shows degenerate Wannier functions as a result of the much lower symmetry. The lowest five Wannier functions maintain the character they had in the parent compound, albeit distortion occurs because of the lowering in symmetry as exemplified in Figure 6a, b. Wannier

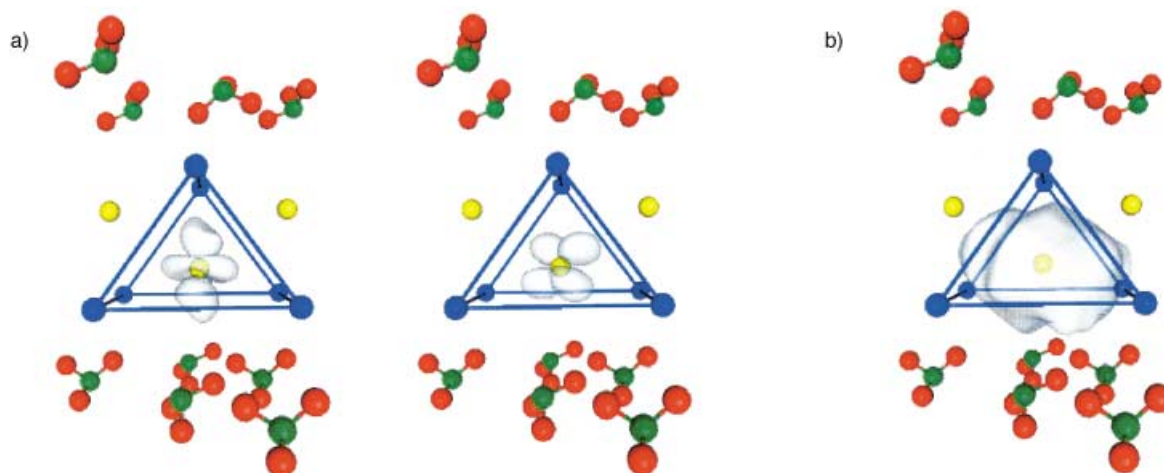


Figure 6. Densities of Wannier states of $\text{CsAu} \cdot \text{NH}_3$. a) Two representatives of the lowest five Wannier functions which maintain the s+d character they had in CsAu . b) High-energy Wannier function losing the d character and resembling more a distorted s state. For color code see Figure 1.

function six, on the other hand, which is the highest in energy, is substantially changed; its spread is significantly larger and its center is slightly shifted from the gold atom by 0.108 \AA in the direction of the nearest ammonia layer, losing the d character and resembling a slightly distorted s state. We believe that it is this particular state which is responsible for many of the properties of $\text{CsAu} \cdot \text{NH}_3$. However, this static calculation cannot shed any light on the nature of the bipolaronic states as suggested by the NMR spectrometry results.

In summary, the intercalation of ammonia (in a formal sense) into CsAu reduces the coulomb field exerted by the cesium ions on the gold centers, which destabilizes the negatively charged state. As a consequence some electron density is removed from the gold site. This picture is in accordance with all the experimental findings, as there are formation of (weak) gold–gold bonds, shift of the Mössbauer signal, and broadening and shift of the NMR signal of the Cs centers.

Experimental Section

All manipulations were carried out either under dry argon, in vacuum, or under an atmosphere of ammonia. Ammonia (Bayer AG, Leverkusen, Germany) was made anhydrous by condensing it first on sodium, then on potassium, where it was stored as a potassium–ammonia solution at 195 K until usage. Cesiumauride was synthesized directly from the elements at 493 K by using an excess of alkali metal which was distilled off in the dynamic vacuum of a mechanical oil pump on completion of the reaction. Cesium was gained by reducing its chloride with calcium^[21] and further purified by twofold distillation under vacuum. Elemental gold was precipitated by reducing tetrachloric gold acid with sodium oxalate.^[22]

In an H-shaped all-glass reaction vessel with its two legs separated in the middle by a glass frit (porosity 2), CsAu was placed on the one side and liquid ammonia was condensed onto it (at $T = 175 \text{ K}$). The CsAu was dissolved by warming to the boiling point of ammonia, then the solution was poured through the glass frit. Upon slow evaporation of the solvent intense blue colored crystals of $\text{CsAu} \cdot \text{NH}_3$ precipitated—which evolved ammonia, after the solvent was removed, at $225 \pm 5 \text{ K}$. This procedure was repeated until all the CsAu was recrystallized.

For selecting and mounting single crystals we have adapted the technique described by Kottke and Stalke.^[23] For all other analytical investigations the ammoniate was synthesized from CsAu and NH_3 directly in the respective

silica sample containers which were sealed under vacuum (the samples were cooled in liquid nitrogen during this procedure to prevent decomposition).

Received: August 21, 2001 [Z17769]

- [1] P. Pykkö, *Chem. Rev.* **1988**, 88, 563–594.
- [2] a) C. Feldmann, M. Jansen, *Angew. Chem.* **1993**, 105, 1107–1108; *Angew. Chem. Int. Ed. Engl.* **1993**, 32, 1049–1050; b) C. Feldmann, M. Jansen, *Z. Anorg. Allg. Chem.* **1995**, 621, 1907–1912; c) The Chemistry of Gold Oxides: M. Jansen, A.-V. Mudring in *Gold—Progress in Chemistry, Biochemistry and Technology* (Ed.: H. Schmidbaur), Wiley-VCH, Weinheim, **1999**, pp. 747–793.
- [3] P. P. Edwards, *Adv. Inorg. Chem.* **1982**, 25, 135–185.
- [4] C. Feldmann, M. Jansen, *J. Chem. Soc. Chem. Commun.* **1994**, 1045–1046.
- [5] Crystal data for $\text{CsAu} \cdot \text{NH}_3$: monoclinic, space group $C2/c$ (no. 15), $a = 721.1(1)$, $b = 703.55(9)$, $c = 1682.6(4) \text{ pm}$, $\beta = 102.37(1)^\circ$, $V = 833.8(3) \times 10^6 \text{ pm}^3$, $\rho_{\text{calcd}} = 5.527 \text{ g cm}^{-3}$, $Z = 8$, $\mu_{\text{MoK}\alpha} = 43.656 \text{ mm}^{-1}$, $F(000) = 1152$, $\lambda = 71.073 \text{ pm}$, Stoe IPDS, graphite monochromator, $T = 123 \text{ K}$, 7161 measured reflexions, 1110 symmetry independent reflexions, final $R1 = 0.0484$, $wR2 = 0.1248$ for 878 observed reflexions ($I_{\text{obs}} > 2\sigma$). The structure solution (heavy atoms) was using direct methods. Subsequent difference Fourier analysis provided the positions of the nitrogen atoms. The hydrogen atoms were localized and refined using a riding model. Further details on the crystal structure investigation(s) may be obtained from the Fachinformationszentrum Karlsruhe, D-76344 Eggenstein-Leopoldshafen, Germany (fax: (+49) 7247-808-666 (Frau S. Höhler-Schlimm); e-mail: crysdata@fiz-karlsruhe.de), on quoting the depository number CSD-412194.
- [6] A.-V. Mudring, M. Jansen, *Angew. Chem.* **2001**, 112, 3194–3196; *Angew. Chem. Int. Ed. Engl.* **2001**, 39, 3066–3067.
- [7] A. Sommer, *Nature* **1943**, 152, 215.
- [8] U. Zachwieja, *Z. Anorg. Allg. Chem.* **1993**, 619, 1095–1097.
- [9] “Beiträge zur Chemie von Polyanionen der 5. Hauptgruppe”: N. Korber, Habilitationsschrift, Bonn, **1997**.
- [10] F. E. Wagner, A.-V. Mudring, M. Jansen, unpublished results.
- [11] J. L. Carolan, T. A. Scott, *J. Magn. Reson.* **1970**, 2, 243–258.
- [12] G. A. Tinelli, D. F. Holcomb, *J. Solid State Chem.* **1978**, 25, 157–168.
- [13] R. Dupree, W. Freyland, W. W. Warren, Jr., *Phys. Rev. Lett.* **1980**, 45, 130–133.
- [14] R. Dupree, D. J. Kirby, W. W. Warren, Jr., *Phys. Rev. B* **1985**, 31, 5597–5603.
- [15] T. R. Hughes, Jr., *J. Chem. Phys.* **1963**, 38, 202–209.
- [16] “Magnetism and Magnetic Resonance across the Metal-Insulator-Transition”: P. P. Edwards in *Physics and Chemistry of Electrons and Ions in Condensed Matter* (Eds.: J. V. Acrivos, N. F. Mott, A. D. Yoffe), D. Reidel, Dordrecht, **1983**, pp. 297–333.

- [17] T. Butz, *Nuclear Spectroscopy on Charge Density Wave Systems*, Kluwer, Dordrecht, 1992.
- [18] R. K. Harris, B. E. Mann, *NMR and the Periodic Table*, Academic Press, London, 1978, chap. 6, pp. 129–181.
- [19] a) The calculation was performed using the plane-wave pseudopotential scheme as implemented in the CPMD code.^[19b] We have used the code CPMD, J. Hutter and co-workers, MPI für Festkörperforschung und IBM Zurich Research Laboratory 1995–1999. Norm-conserving pseudopotentials of the Martin Trouiller type^[19c] were employed and the Kohn and Sham orbitals were expanded up to an energy cutoff of 60 Ry. We use only the Γ point of the supercell of 48 and 16 atoms for CsAu·NH₃ and CsAu, respectively; b) R. Car, M. Parrinello, *Phys. Rev. Lett.* **1985**, 55, 2471–2474; c) N. Trouiller, J. L. Martins, *Phys. Rev. B* **1991**, 43, 1993–2006.
- [20] a) N. Marzani, D. Vanderbilt, *Phys. Rev. B* **1997**, 56, 12847–12865. The maximally localized Wannier functions w_i as introduced by Marzani and Vanderbilt are obtained by a unitary transformation U_{ij} in the subspace of the occupied Kohn and Sham orbitals Ψ_j , $w_i = \sum_j U_{ij} \Psi_j$ by imposing that the spread function $S = \sum_i (\langle w_i | r^2 | w_i \rangle - \langle w_i | r | w_i \rangle^2)$ is minimal; they are the highly nontrivial generalization to a periodic system of the Boys orbitals.^[20b] Very efficient algorithms have been implemented to carry out the minimization of S .^[20c] b) S. F. Boys, *Quantum Theory of Atoms, Molecules and the Solid State* (Ed.: P. O. Lowdin), Academic Press, New York, 1996, p. 253; c) G. Berghold, C. J. Mundy, A. H. Romero, J. Hutter, M. Parrinello, *Phys. Rev. B* **2000**, 61, 10040–10048.
- [21] L. Hackspill, *Helv. Chim. Acta* **1928**, 11, 1008.
- [22] L. Vanino, *Handbuch der Präparativen Anorganischen Chemie*, Vol. 1, Enke, Stuttgart, 1921, p. 520.
- [23] T. Kottke, D. Stalke, *J. Appl. Crystallogr.* **1993**, 26, 615–619.

High-Throughput Screening of Enantioselective Catalysts by Immunoassay

Frédéric Taran, Cécile Gauchet, Barbara Mohar, Stéphane Meunier, Alain Valleix, Pierre Yves Renard, Christophe Créminon, Jacques Grassi, Alain Wagner,* and Charles Mioskowski*

Interest is continuously growing in the application of powerful combinatorial approaches to the discovery of new catalysts by combining synthesis and screening of large libraries.^[1] Although this area is still in its infancy, several catalysts have already been identified by parallel synthesis

[*] Dr. A. Wagner, Dr. C. Mioskowski, Dr. B. Mohar
Université Louis Pasteur, Laboratoire de Synthèse Bioorganique
(UMR 7514), 74, route du Rhin 67401 Illkirch-Graffenstaden (France)
Fax: (+33) 3-90-24-43-06
E-mail: wagner@bioorga.u-strasbg.fr
mioskowski@aspirine.u-strasbg.fr

Dr. F. Taran, C. Gauchet, S. Meunier, A. Valleix, Dr. P. Y. Renard
Service des Molécules Marquées
DBCM/DSV CEA Saclay 91191 Gif sur Yvette Cedex (France)

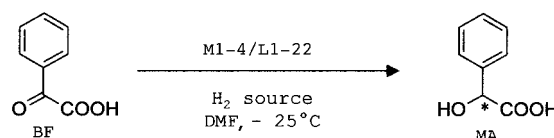
Dr. C. Créminon, Dr. J. Grassi
Service de Pharmacologie et d'Immunologie, DRM/DSV CEA Saclay
91191 Gif sur Yvette Cedex (France)

Supporting information for this article is available on the WWW under <http://www.angewandte.com/> or from the author.

and high-throughput-screening (HTS) techniques.^[2] However, the factor limiting an efficient extension of this research to asymmetric catalysis remains the lack of efficient methods for rapid screening of enantioselective reactions.^[3] To overcome this major obstacle, a first approach consists in screening the catalyst library for activity using an HTS procedure and then testing each lead for enantioselectivity by conventional methods,^[4] but this is only amenable if few catalysts from the broad library are active. Clearly, a high-throughput technique allowing quantification of both activity and enantioselectivity would accelerate the rate at which asymmetric catalysts are discovered. Recently, IR thermography,^[5] capillary array electrophoresis,^[6] CD-HPLC,^[2c] and electrospray ionization based on the use of isotopically labeled substrates^[7] have emerged as promising but equipment-intensive techniques for the screening of enantioselective catalysts.^[8]

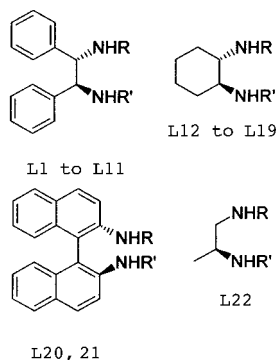
Herein, we describe a new HTS method for the simultaneous screening of multiple catalysts for the enantioselective reduction of ketones. This procedure, allows quantification of both yields and enantiomeric excess (*ee*) in an HTS format using inexpensive and commonly available equipment.

Our interest in this field was focused on the enantioselective reduction of α -keto acids by hydrogen transfer using chiral metal complexes. Although considerable effort was expended to develop applicable methods for the enantioselective preparation of α -hydroxy acids,^[9] only a few papers^[10] are devoted to the development of straightforward procedures involving the direct conversion of α -keto acids to chiral α -hydroxy acids. As a model reaction, we chose the enantioselective reduction of benzoyl formic acid (BF) into mandelic acid (MA). The catalyst library was prepared by combining a set of 22 chiral diamine-based ligands and four different metal species (Scheme 1).



Metal library:
M1 : [RuCl₂(*p*-cym)]₂
M2 : [RuCl₂(benz)]₂
M3 : [RhCl₂(Cp)]₂
M4 : [IrCl₂(Cp)]₂

Ligand library:



L	R	R'
1	H	H
2	CF ₃ SO ₂	H
3	C ₆ F ₅ SO ₂	H
4	4-CF ₃ C ₆ H ₄ SO ₂	H
5	2, 4, 6-CH ₃ C ₆ H ₂ SO ₂	H
6	4-CH ₃ C ₆ H ₄ SO ₂	H
7	C ₆ F ₅ SO ₂	H
8	CF ₃ CO	H
9	C ₆ H ₅ CO	H
10	4-CH ₃ C ₆ H ₄ SO ₂	4-CH ₃ C ₆ H ₄ SO ₂
11	C ₆ H ₅ CH ₂ CO ₂	C ₆ H ₅ CH ₂ CO ₂
12	H	H
13	CF ₃ SO ₂	H
14	C ₆ F ₅ SO ₂	H
15	4-CH ₃ C ₆ H ₄ SO ₂	H
16	2, 4, 6-CH ₃ C ₆ H ₂ SO ₂	H
17	4-CF ₃ C ₆ H ₄ SO ₂	H
18	CF ₃ SO ₂	CF ₃ SO ₂
19	CH ₃ SO ₂	CH ₃ SO ₂
20	H	H
21	CF ₃ SO ₂	H
22	H	H

Scheme 1. Target reaction and catalyst library.